Estimation of Intersegmental Load at L5-S1 during Lifting/Lowering Tasks Using Force Plate Free Markerless Motion Capture

Jindong Jiang [a,b], Wafa Skalli[a], Ali Siadat[b], Laurent Gajny[a]

[a] Arts et Metiers Institute of Technology, Institut de Biomecanique Humaine Georges Charpak, 151 Boulevard de l'Hôpital, 75013 Paris, France

[b] Arts et Metiers Institute of Technology, Laboratoire de Conception Fabrication Commande, 4 Rue Augustin Fresnel, 57070 Metz, France

Corresponding Author:

Laurent Gajny / laurent.gajny@ensam.eu

Abstract

Accurate estimation of joint load during a lifting/lowering task could provide a better understanding of the pathogenesis and development of musculoskeletal disorders. In particular, the values of the net force and moment at the L5-S1 joint could be an important criterion to identify the unsafe lifting/lowering tasks. In this study, the joint load at L5-S1 was estimated from the motion kinematics acquired using a multi-view markerless motion capture system without force plate. The 3D human pose estimation was first obtained on each frame using deep learning. The kinematic analysis was then performed to calculate the velocity and acceleration information of each segment. Then, the net force and moment at the L5-S1 joint were calculated using inverse dynamics with a top-down approach. This estimate was compared to a reference with a bottom-up approach. It was computed using a marker-based motion capture system combined with force plates and using personalized body segment inertial parameters derived from a 3D model of the human body shape constructed for each subject using biplanar radiographs. The average differences of the estimates for force and

moment among all subjects were 14.0 ± 6.9 N and 9.0 ± 2.3 Nm, respectively. Meanwhile, the mean peak value differences of the estimates were 10.8 ± 8.9 N and 11.9 ± 9.5 Nm, respectively. This study then proposed the most rigorous comparison of mechanical loading on the lumbar spine using computer vision. Further work is needed to perform such an estimation under realistic industrial conditions.

Keywords: Inverse dynamic, markerless, deep learning, human pose estimation, ergonomics

1 Introduction

Approximately 1.71 billion people worldwide suffer from musculoskeletal disorders (MSDs) (Cieza et al. 2020). Low-back pain is one of the most common MSDs and the lower back is particularly vulnerable to lifting (Mohd Nur et al. 2018). The causal link between mechanical loads and low back pain (LBP) has been well established (Skals et al. 2021; Ghezelbash et al. 2020; Griffith et al. 2012; McAtamney and Nigel Corlett 1993; Coenen et al. 2014), despite the fact that this relationship has faced some controversy due to several recent conflicting findings (Swain et al. 2020).

Prevention of work-related MSDs in industry is carried out using ergonomic assessments such as the Rapid Upper Limb Assessment (RULA) (McAtamney and Nigel Corlett 1993). The RULA score is mainly based on joint angles assessed by ergonomists using observational analysis. The risk indicators correspond to a wide range of joint angles, which can lead to specificity problems. On the other hand, observational analysis can lead to reproducibility problems. Quantitative biomechanical analysis using motion capture could then help to solve the problems of current ergonomic analysis.

Marker-based motion capture, usually combined with force plates, can provide accurate

kinematic and kinetic analysis, but it is not well suited for ergonomic assessment in industrial routine. In fact, it can cause several hindrances to the workers' activities, it requires human resources and a lot of hardware. Therefore, force plate-free markerless motion capture can be a relevant alternative in this context. Many researches are available for kinematic analysis using markerless motion capture (Cronin 2021; Kanko et al. 2021; Vafadar et al. 2022) but the researches for kinetic analysis are less abundant.

There are two main paradigms for calculating intersegmental loads, the top-down approach and the bottom-up approach. The top-down model starts from the head, while the bottom-up model starts from the feet. Unlike the bottom-up approach, the top-down approach does not require a force platform to measure ground reaction forces, making it more suitable for markerless motion capture systems. To validate the accuracy of the estimated joint load at L5-S1 from a force platform-free markerless motion capture system, some studies have compared the results between marker-based and markerless systems using the bottom-up approach (Kanko et al. 2023; Song et al. 2023; Tang et al. 2024) but force plates may not be available in industrial environments. On the other hand, (Mehrizi et al. 2019) used the top-down approach for their evaluation. However, the accuracy of the reference values remains unclear because the L5-S1 load calculated by the bottom-up approach is closer to the true value (Kingma et al. 1996).

The estimation of the body segment inertial parameters (BSIPs) is fundamental in this kinetic analysis, and the classical method proposed by (de Leva 1996) is usually used to obtain the inertial information of each segment, such as length, mass, the center of mass, and inertia matrix, by using the information of the joint position, the subject's gender, and the total body

mass as inputs. However, this method does not take into account the individual anthropometric measurements of the subject's body. Therefore, numerous studies (Dumas et al. 2006; Kollia et al. 2012; Pillet et al. 2010; Robert et al. 2017; Venture et al. 2019) have been conducted to compute the personalized BSIPs to improve the accuracy of intersegmental loads. In (Pillet et al. 2010), the authors reported better accuracy in estimating the center of pressure using personalized BSIPs rather than anthropometric tables, but they used a body shape modeling method that lacked accuracy. Barycentremetry using biplanar radiographs allows for an accurate estimation (Nérot et al. 2015; Sandoz et al. 2010) but it is not applicable in routine work environment.

The aim of this paper was then to propose a force plate-free top-down approach, based on the markerless system presented in (Vafadar et al. 2022; Vafadar et al. 2021), to estimate the intersegmental load at L5-S1 during the lifting/lowering tasks using a multiview markerless motion capture system. The proposed method was evaluated by comparison with a reference method using a marker-based motion capture system coupled with a force plate and with accurate subject-specific BSIP computed using barycentremetry.

2 Materials and methods

2.1 Participants

The experiment took place in 2021 and 2022 with volunteer asymptomatic participants. Exclusion criteria for the subjects included pregnancy, a diagnosed spinal disorder, and inability to read French. Twelve subjects (24.2 ± 2.3 years, 172.4 ± 10.1 cm, 65.9 ± 14.7 kg) participated in the experiment. The experiment was approved by the ethics committee (CPP 06036, Ile de France VI). All subjects have signed an informed consent form. Before the

experiment, a medical examination was performed by an orthopedic surgeon to determine the subject's ability to perform the experiment. If able, a short and individualized warm-up period was recommended by the physician.

2.2 Data acquisition

For details on data acquisition, refer to (Vafadar et al. 2022; Vafadar et al. 2021). For clarity, the most important information is summarized below.

Two different systems were used to record motion: a reference marker-based system (Vicon, UK) synchronized with a force platform and a markerless system with four digital cameras (GoPro Hero 7 Black) (Vafadar et al. 2022; Vafadar et al. 2021; Jiang et al. 2022).

To simulate industrial lifting tasks, subjects were asked in a laboratory environment to lift a cardboard box onto a table and then to lower it. Different movement types (lifting, lowering), lifting heights (73 cm,125 cm), and asymmetric angles (0°, 45°, 90°, to the left) were included in the experiment. Each action was repeated twice, for a total of 24 (2 × 2 × 2 × 3) trials, lasting approximately 8 minutes. Of all the subjects, S01 carried a larger cardboard box (weight: ≈0kg, size: 60.0*40.0*40.0cm) while the others carried a smaller box (weight: 5kg, size: 42.0*32.0*36.0cm). The data corresponding to S01 was included in the test set (Jiang et al. 2024).

A total of 181,624 frames were acquired during the experiment. Among them, 540 frames with missing markers and 804 frames with camera occlusion were excluded from the dataset. Therefore, 180,820 frames were used for model training and testing. Each frame has four camera views with corresponding camera intrinsic and extrinsic parameters. To protect the privacy of the subjects, their faces were blurred in the image set (Jiang et al. 2022). A learnable

triangulation neural network (Iskakov et al. 2019) was trained/evaluated on the dataset for 3D human pose estimation, where 6 subjects were randomly selected as the training set and the rest were in the test set. In addition, biplanar X-rays (EOS Imaging, ATEC Spine, Carlsbad, CA, USA) were collected and 3D reconstruction of the body shape were performed (Nérot et al. 2015).

2.3 Inverse dynamics

Based on the human pose estimation with stereovision, inverse dynamics was used to calculate the load on body joint L5-S1, exploring top-down and bottom-up paradigms.

2.3.1 Body segment's inertial parameters

After the 16 joints from the multi-view stereo system, the human body model was constructed as a linked chain consisting of 10 rigid body segments, with forearms, upper arms, head, trunk, thighs and shanks. Two methods were used to calculate the body inertia parameters (BSIPs), namely the proportional method and the geometric method.

In the proportional method, the inertial properties of each body segment were calculated using the approach proposed by (de Leva 1996). The input to the method is the subject's gender and body mass, which yields the position of the segment's center of mass, the segment's mass, and the inertia tensor with respect to the central inertia principal axis.

In the geometric method, based on the biplanar radiographs collected in the experiment, a personalized 3D digital model of the human body was created for each subject in this work using the method described in (Nérot et al. 2015). The result is a 3D human body envelope which can be used to calculate the BSIPs. It should be noted that the biplanar radiographs were

only used in the calculation of the reference value for comparison. The 3D digital model was segmented into different body segments, after which the mass, center of mass, and inertia of each segment were calculated based on the human body density data given by (Dempster 1955), with the thorax density updated according to (Amabile et al. 2016). A sample of biplanar radiographs and the corresponding 3D body shape are shown in Figure 1.

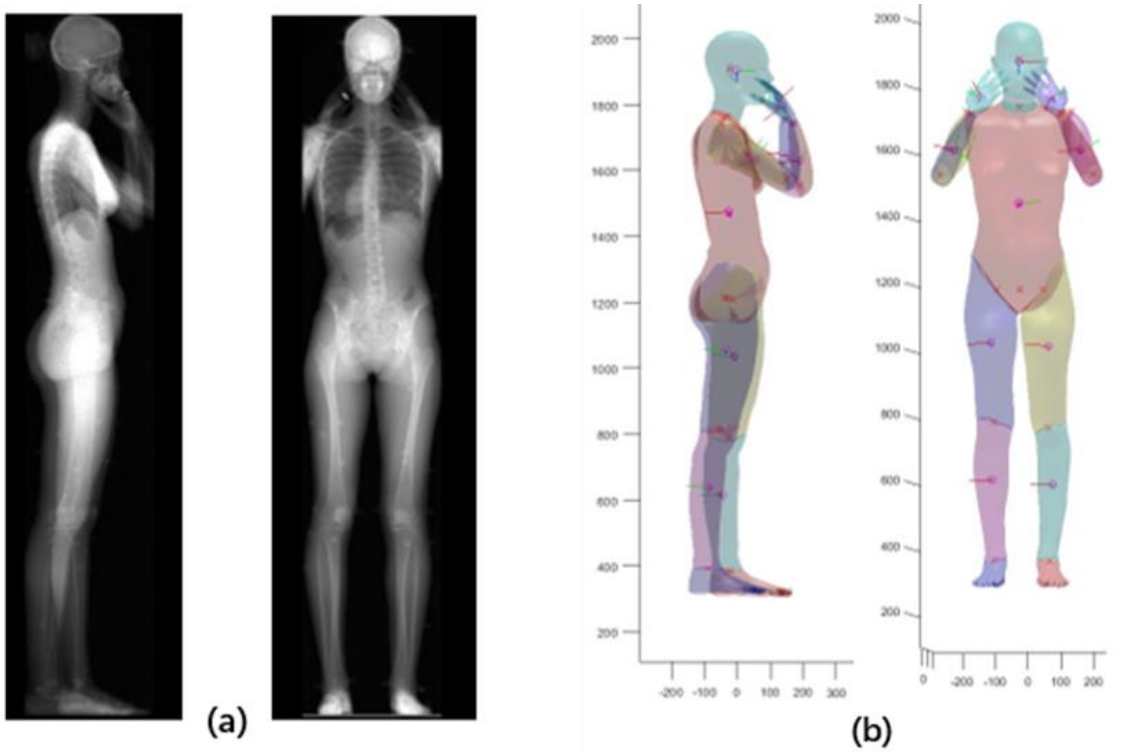

Fig. 1. (a) Sample images of low-dose biplanar X-ray radiographs; (b) 3D human body shape based on radiography. Each segment is distinguished by a different color. The red circle on each segment represents the center of mass, and the axes represent its inertial principal axis, with the length indicating the relative magnitude of the rotational inertia about the corresponding axis. The red crosses denote the body key points, which are used for the localization of the center of mass position.

2.3.2 Kinematic calculations

Based on the joint positions obtained from the 3D human pose estimation, we performed the kinematic analysis to calculate the velocity and acceleration information of each segment. Specifically, the motion data were filtered using a fourth-order Butterworth low-pass filter with a cutoff frequency of 2.5 Hz. The center of mass acceleration was calculated using the second order differentiation of the center of mass position with respect to time. For the angular

acceleration, we first calculated the helical axis and angular velocity using the finite difference of the rotation matrix, and then differentiated the angular velocity with respect to time to obtain the angular acceleration.

2.3.3 External Forces

In addition to gravity, the force exerted on a human segment by an external object other than the human segments is considered an external force. In the process of handling the cardboard box, the main external forces were the ground reaction force on the subject's foot which was measured by a force platform, and the force from the cardboard box on the hands.

The force exerted by the box on the hand was calculated from the mass and acceleration of the box. The mass of the box itself was negligible and ignored in the following calculation. During the experiment, a metal disk (mass = 5kg, radius = 10cm, height = 2cm) was placed inside the box. The acceleration of the subject's wrists was calculated and used to approximate the acceleration of the box. During the process of lifting, when the box was just starting to move, the support force on the box from the ground/table was the weight of the box. When the box was completely off the floor, the support force became 0. Although there was a transition period between these two states, the change in support force was simplified to be completed instantaneously at the moment the box began to move. The same simplification was made for the phase of placing the boxes on the ground/table. The time labels at which the boxes started to move or completely stopped were manually annotated and verified using the motion data of the markers on the box.

2.3.4 Inverse dynamics

Based on the above calculations, the loads on the subject's joints at L5-S1, including the forces as well as the moments, were calculated as follows:

$$F_{L5S1} = -F_r + \sum_{i=1}^{k}(-m_i g + m_i a_i) \quad (2\text{-}1)$$

$$M_{L5S1} = \Gamma_r - (r_r - r_{L5S1}) \times F_r + \sum_{i=1}^{k}[(r_i - r_{L5S1}) \times (-m_i g + m_i a_i)] + \sum_{i=1}^{k}\Gamma_i^I \quad (2\text{-}2)$$

$$\Gamma_i^I = R_i'(I_i'\alpha_i' + \omega_i' \times (I_i'\omega_i')) \quad (2\text{-}3)$$

where F_{L5S1} and M_{L5S1} denote the intersegmental forces/moments acting on the joint L5-S1. F_r and r_r are the external force exerted on human segments and the vector to its point of application. Γ_r is an external free moment. r_i and r_{L5S1} are the vectors to the center of mass (COM) of segment i and L5-S1 joint, respectively. m_i and I_i' are the mass of the segment i and the inertial tensors in the segment local coordinate system. a_i is the translational acceleration of the COM in the global coordinate system. α_i' and ω_i' are the angular acceleration and velocity of segment i. g is the gravitational acceleration. Γ_i^I is the inertial contribution of segment i in the global coordinate system. R_i' is the rotation matrix that transform the coordinates of the vector from the local coordinate system of segment i to global coordinate system.

2.3.5 Evaluation

In this study, we used a bottom-up L5-S1 load estimation method to validate our top-down

estimates. The bottom-up method was implemented to provide the reference values of L5-S1 load which were then compared with estimates from the top-down approach. The computational procedure starts from the foot, up along the kinetic chain. The resultant of all the forces on the lower section is calculated, and the equilibrium equations for the lower section give the resultant of the generalized forces at L5-S1 (equal and opposite). The reaction forces and the free moments from the ground on the subject's feet, measured by a force platform, were used to initiate the calculation. To enhance the calculation accuracy of L5-S1 load reference, the geometric models reconstructed from biplanar radiographic were employed for the BSIPs calculation. In order to evaluate the accuracy of the markerless and plateform-less L5-S1 load estimates, we calculated the component differences between the estimates and the reference along each direction, as well as the difference between their Euclidean norms (i.e., vector modulus). Mean and standard deviation of the Root Mean Squared Differences (RMSD) and peak-value differences for each trial were calculated for each subject. Global mean and standard deviation on all subject were calculated as a global measure of the agreement between the two methods. This evaluation was lead on the 6 subjects of our test set, resulting in 91,255 sampling values.

3 Results

The load estimates of L5-S1 with the reference values during the subject's lifting and lowering trials, respectively, including the force and moment components in each orientation and their Euclidean norms, were visualized for qualitative evaluation (See Figure 2 and 3). Each of these results represents the loads on a given subject during a specific lifting or lowering trial. It was observed that the estimated values of the loads were in good agreement with the

reference values. In addition, the components of the force in the vertical and anterior-posterior directions were relatively large, while the components in the lateral direction are small. The moment has a relatively large component in the sagittal plane and a moderate component in the coronal plane, with a considerably smaller component in the transverse plane. At the beginning or end of the handling action, the component of the force in the vertical direction was relatively large, while the component of the force in the other directions was approximately zero and the component of the moment in each direction was also nearly zero. Meanwhile, we noted that there were two sharp variations in the load estimates. For smaller load components in some planes, such as the moment in the transverse plane, the pattern of the load estimate may differ from that of the reference value.

The average RMSD (± standard deviation) of the estimates for force and moment across subjects were 14.0 ± 6.9 N and 9.0 ± 2.3 Nm, respectively (see Table 1). Smaller mean differences were observed for moment estimates in the transverse plane than in the frontal and sagittal planes. The mean RMSD per subject ranged between 7 N and 30 N for forces and between 3 Nm and 12.5 Nm for moments.

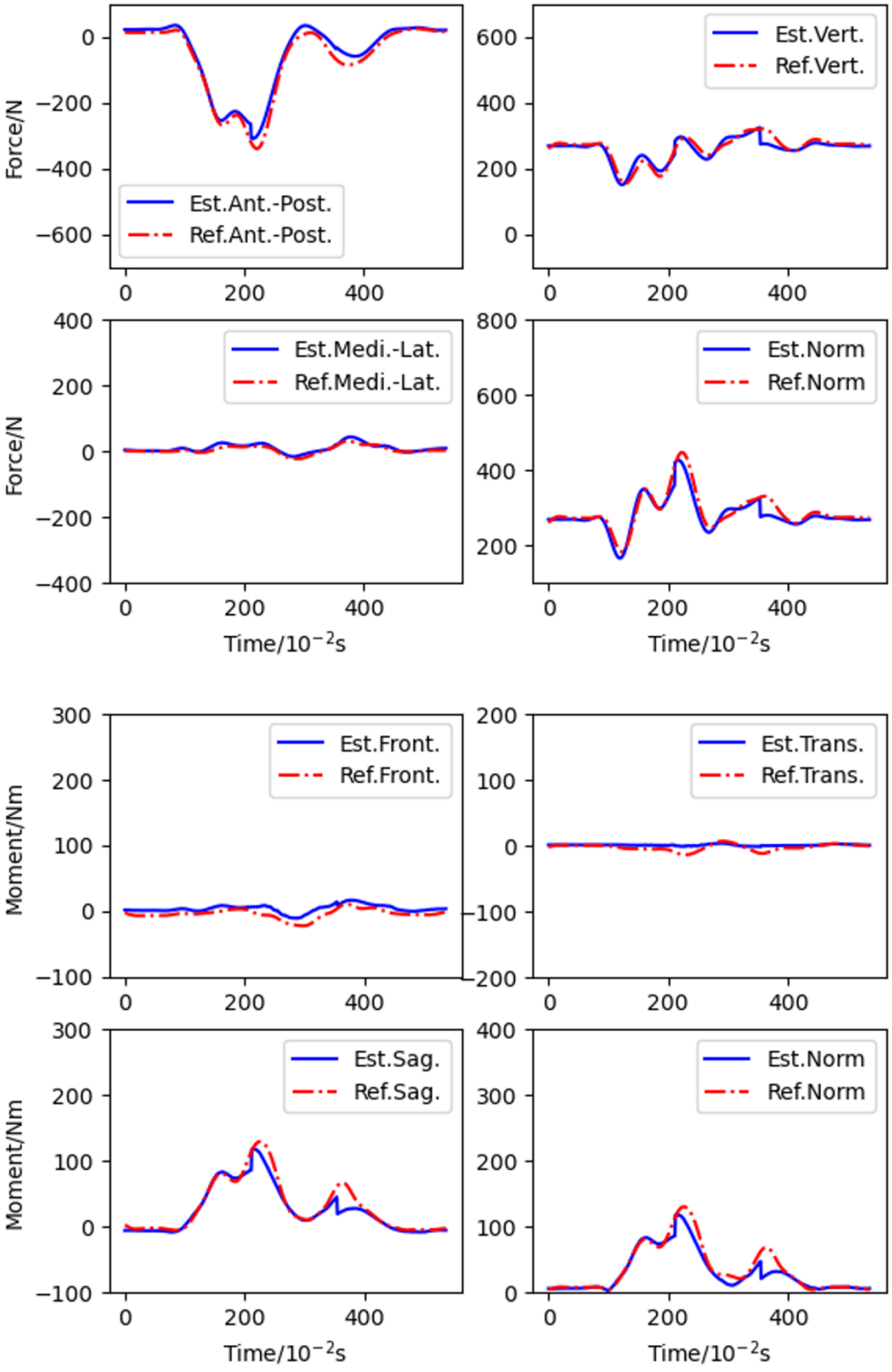

Fig. 2. Example result of L5-S1 load versus time during a lifting task (subject ID: S02, task trial: #19). Est.=estimate, Ref.=reference, Ant.-Post=anteroposterior, Vert.=vertical, Medi.-Lat.= mediolateral , Front. =frontal plane, Trans.= transverse plane, Sag. = sagittal plane, Norm= Euclidean norm.

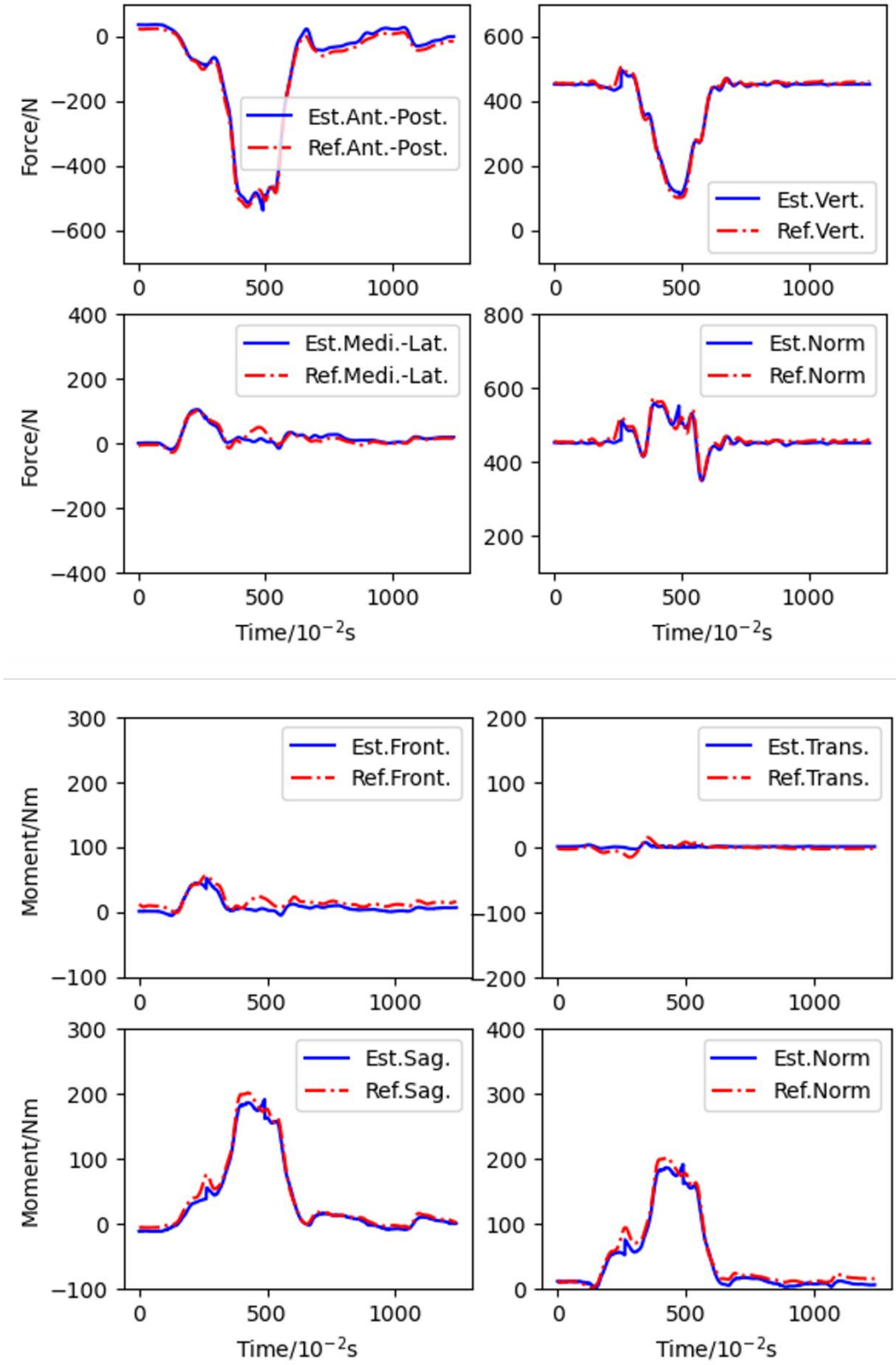

Fig. 3. Example result of L5-S1 load versus time during a lowering task (subject ID: S04, task trial: #00). Est.=estimate, Ref.=reference, Ant.-Post=anteroposterior, Vert.=vertical, Medi.-Lat.= mediolateral , Front. = frontal plane, Trans.= transverse plane, Sag. = sagittal plane, Norm= Euclidean norm.

The mean peak value differences (± standard deviation) of the estimates for force and moment among all subjects were 10.8 ± 8.9 N and 11.9 ± 9.5 Nm, respectively (see Table 2). Larger differences were observed in the mediolateral component for force estimates and in the sagittal plane for moment estimates. S01 evidenced substantially higher peak value differences for the medio-lateral component of force estimates which is explained by large occlusions because of the larger box used for the experiment with this subject.

Table 1. RMSD of the difference between the reference and estimate of L5-S1 load for each subject across the trials. Ant.-Post=anteroposterior, Vert.=vertical, Medi.-Lat.= mediolateral , Front. = frontal plane, Trans.= transverse plane, Sag. = sagittal plane, Norm= Euclidean norm.

		Force (N)				Moment (Nm)			
subject	statistics	Ant-Post	Vert.	Medi.-Lat	Norm	Front.	Trans.	Sag.	Norm
S01	μ	17.5	17.6	19.2	12.8	10.3	3.3	10.2	8.1
	σ	5.6	3.8	10.2	3.3	2.2	0.6	1.9	1.3
S02	μ	9.4	10.5	13.9	9.7	10.9	6.3	8.4	9.1
	σ	1.3	1.5	2.9	1.9	1.5	2.0	1.1	1.1
S03	μ	16.3	12.8	16.4	13.0	8.1	5.3	11.7	10.3
	σ	1.8	1.4	5.1	1.7	2.0	2.1	1.5	1.2
S04	μ	16.0	9.2	12.1	9.4	7.9	4.9	12.4	11.8
	σ	1.1	1.5	4.0	1.6	1.4	1.5	2.5	2.0
S05	μ	12.8	24.8	12.8	27.9	8.2	3.3	7.6	6.6
	σ	1.8	0.8	1.6	0.6	0.8	0.9	1.4	1.5
S06	μ	7.2	9.6	13.1	10.9	6.4	3.3	7.1	7.4
	σ	1.0	1.6	3.2	1.4	1.6	1.5	1.1	1.0
All	μ	12.8	13.7	14.1	14.0	8.5	4.5	9.5	9.0
	σ	4.2	6.0	4.9	6.9	2.2	2.0	2.6	2.3

Table 2. Peak value difference between the reference and estimate of L5-S1 load for each subject across the trials. Ant.-Post=anteroposterior, Vert.=vertical, Medi.-Lat.= mediolateral , Front. = frontal plane, Trans.= transverse plane, Sag. = sagittal plane, Norm= Euclidean norm.

		Force				Moment			
subject	statistics	Ant-Post	Vert.	Medi.-Lat	Norm	Front.	Trans.	Sag.	Norm
S01	μ	6.3	5.6	27.6	5.2	12.6	3.3	15.2	14.8
	σ	2.3	2.8	24.4	2.7	5.6	1.5	4.8	5.2
S02	μ	2.8	3.8	10.1	3.0	10.0	7.9	13.0	13.2
	σ	2.8	3.4	6.4	3.6	7.0	5.9	6.1	6.8
S03	μ	14.9	9.3	10.2	15.1	4.7	7.3	13.9	14.1
	σ	11.9	8.0	6.6	11.3	5.1	2.8	10.0	10.0
S04	μ	11.1	6.0	12.4	10.1	5.3	6.3	23.4	23.6
	σ	6.2	4.5	9.8	5.3	3.7	3.5	6.6	6.3
S05	μ	15.0	21.3	14.7	19.6	10.0	5.5	3.3	3.8
	σ	7.4	5.8	8.1	6.3	4.4	3.3	2.8	3.0
S06	μ	8.8	4.7	7.7	9.0	3.5	6.9	2.8	3.3
	σ	7.0	3.2	6.2	7.3	2.1	6.0	2.1	2.1
All	μ	10.1	8.7	12.4	10.8	7.2	6.5	11.6	11.9
	σ	8.5	8.0	11.0	8.9	5.7	4.5	9.5	9.5

4 Discussion

The purpose of this study was to estimate and evaluate the intersegmental forces/moments at the L5-S1 joint calculated using a multiview forceplate-free markerless motion capture system. The reference value and the estimated value of the load used completely independent calculation strategies, with the considered body segments and the external forces being completely. The reference value was computed using inverse dynamics with a bottom-up approach and subject-specific BSIPs derived from a 3D model of the body shape obtained from biplanar radiographs. On the other hand, the estimated value was computed using inverse dynamics and a top-down approach. The mean differences in force and moment estimates across subjects were 14.0 ± 6.9 N and 9.0 ± 2.3 Nm, respectively, providing solid evidence for

the reliability of these estimates.

The reference values against which our estimates were compared cannot be considered as actual ground truth, as they are not easily available in vivo. Bottom-up inverse dynamics, with or without subject-specific BSIPs, is an imperfect modeling method. However, it is commonly used in similar studies (Faber et al. 2016; Pillet et al. 2010) and provides feasible values. Moreover, for simple movements such as those studied in this paper, it is also possible to interpret the different phases of the movement on the force and moment curves.

Few studies have focused on intersegmental load estimation from markerless motion capture and to the best of our knowledge, only two have focused on force plate-free estimation (Mehrizi et al. 2019; Mehrizi et al. 2017). In these studies, the authors compared their estimate, derived from a 2-camera markerless system, to a reference which has been computed thanks to a marker-based system and top-down inverse dynamics. The average differences in force and moment estimates across subjects were 4.9 ± 4.9 N and 9.0 ± 7.6 Nm respectively. Using the same evaluation strategy for our system, we obtained average differences in estimates for force and moment across subjects of 2.5 ± 0.9 N and 3.2 ± 1.4 Nm respectively. These better performances can be explained by several factors. First, our system has 4 cameras instead of 2. Second, we performed a thorough calibration of the stereovision system using approximately 40 calibration frames with a machined chessboard, ensuring an overall mean reprojection error of 0.06 pixel. Third, the choice of the human pose estimation method can significantly affect the results. In (Mehrizi et al. 2019), they used a 2D pose estimation method with the Hourglass network (Newell et al. 2016) which achieved state-of-the-art performance at the time on a 2D metric (PCKh@0.5) that only gives the percentage of "correctly" detected points. On the other

hand, we chose a 3D pose estimation method that reported an average position difference with a marker-based system of 2 cm. After fine-tuning on a dedicated dataset, we obtained state-of-the-art results with an average localization error of 1.3 cm (Jiang et al. 2022; Vafadar et al. 2021).

This study focused on the L5-S1 joint for several reasons. First, in our human pose estimation method, an associated key point was detected at this level. Thus, this approach does not require musculoskeletal modeling to estimate the other spinal joints. Second, this joint is the most loaded joint during the lifting and lowering task. Third, this joint is the only one that has been studied in similar work and therefore we can compare with their results. However, it should be noted that the load at any other available joint can be estimated using our approach. The final results of the load at L5-S1 were expressed in the local coordinate system of pelvis (Jiang et al. 2022), and therefore the components of L5-S1 have anatomical sense. In addition, the L5-S1 load obtained in this paper can be used to further calculate the pressure intensity of the lumbar spine if the cross-sectional area of the lumbar spine is given.

However, the present study has several limitations. First, it focused on a population consisting only of young healthy adults. As a result, the observed differences in BSIPs between proportional and subject-specific methods are small. Second, it should also be mentioned that the accuracy of the BSIPs calculation with the proportional 3D human model was still limited. To address this issue, a possible solution is that perform digital 3D body model reconstruction of workers based on RGB images, and then calculate BSIPs with the personalized body models. Third, There is no consensus on acceptable differences for the L5-S1 calculation yet, so our results were only compared with existing literature (Mehrizi et al. 2019; Mehrizi et al. 2017).

Finally, the collected dataset (laboratory environment and clothing of the volunteers) was not realistic with the industrial environment and was limited to six subjects only. Moreover, some a priori knowledge (weight of the box) and manual input (detection of the contact time with the box) were necessary to perform the calculation. Further studies are then necessary to validate extensively this approach in a realistic setting.

5 Conclusion

In this study, we used a multiview force plate-free markerless stereovision system together with artificial intelligence technology to estimate the net force and moment at the lower back during lifting and lowering movements. The top-down method was used for estimation with the RGB images, while the bottom-up method was used with the data from the Vicon system and employed as a reference. Promising results were observed for a population with young adults, justifying further expected developments in markerless motion capture for biomechanical and ergonomic studies.

Acknowledgements

The authors would like to thank the Fondation Arts et Métiers for supporting this work and Marc Khalifé, Floren Colloud, Xavier Bonnet, Saman Vafadar and Hélène Pillet for their technical assistance.

References

Amabile, C., Choisne, J., Nérot, A., Pillet, H., Skalli, W.: Determination of a new uniform thorax density representative of the living population from 3D external body shape modeling. J. Biomech. 49, 1162–1169 (2016). https://doi.org/10.1016/j.jbiomech.2016.03.006

Cieza, A., Causey, K., Kamenov, K., Hanson, S.W., Chatterji, S., Vos, T.: Global estimates of the need for rehabilitation based on the Global Burden of Disease study 2019: a systematic analysis for the

Global Burden of Disease Study 2019. The Lancet. 396, 2006–2017 (2020). https://doi.org/10.1016/S0140-6736(20)32340-0

Coenen, P., Gouttebarge, V., van der Burght, A.S.A.M., van Dieën, J.H., Frings-Dresen, M.H.W., van der Beek, A.J., Burdorf, A.: The effect of lifting during work on low back pain: a health impact assessment based on a meta-analysis. Occup. Environ. Med. 71, 871–877 (2014). https://doi.org/10.1136/oemed-2014-102346

Cronin, N.J.: Using deep neural networks for kinematic analysis: Challenges and opportunities. J. Biomech. 123, 110460 (2021). https://doi.org/10.1016/j.jbiomech.2021.110460

Dempster, W.T. (Wilfrid T.: Space requirements of the seated operator : geometrical, kinematic, and mechanical aspects of the body, with special reference to the limbs. (1955)

Dumas, R., Verriest, J.-P., Skalli, W., de Guise, J.: Comparison of Bi-planar Radiography and Adjusted Scaling Equations for the Computation of Appropriate 3D Body Segment Inertial Parameters. SAE Trans. 115, 1165–1170 (2006)

Faber, G.S., Chang, C.C., Kingma, I., Dennerlein, J.T., van Dieën, J.H.: Estimating 3D L5/S1 moments and ground reaction forces during trunk bending using a full-body ambulatory inertial motion capture system. J. Biomech. 49, 904–912 (2016). https://doi.org/10.1016/j.jbiomech.2015.11.042

Ghezelbash, F., Shirazi-Adl, A., Plamondon, A., Arjmand, N.: Comparison of different lifting analysis tools in estimating lower spinal loads – Evaluation of NIOSH criterion. J. Biomech. 112, 110024 (2020). https://doi.org/10.1016/j.jbiomech.2020.110024

Griffith, L.E., Shannon, H.S., Wells, R.P., Walter, S.D., Cole, D.C., Côté, P., Frank, J., Hogg-Johnson, S., Langlois, L.E.: Individual participant data meta-analysis of mechanical workplace risk factors and low back pain. Am. J. Public Health. 102, 309–318 (2012). https://doi.org/10.2105/AJPH.2011.300343

Iskakov, K., Burkov, E., Lempitsky, V., Malkov, Y.: Learnable Triangulation of Human Pose. In: 2019 IEEE/CVF International Conference on Computer Vision (ICCV). pp. 7717–7726. IEEE, Seoul, Korea (South) (2019)

Jiang, J., Skalli, W., Siadat, A., Gajny, L.: Effect of Face Blurring on Human Pose Estimation: Ensuring Subject Privacy for Medical and Occupational Health Applications. Sensors. 22, 9376 (2022). https://doi.org/10.3390/s22239376

Jiang, J., Skalli, W., Siadat, A., Gajny, L.: Towards Biomechanical Analysis in Workplace Ergonomics Using Marker-Less Motion Capture: 3D Human Pose Estimation for Lifting/Lowering Tasks. In: Skalli, W., Laporte, S., and Benoit, A. (eds.) Computer Methods in Biomechanics and Biomedical Engineering II. pp. 179–186. Springer Nature Switzerland, Cham (2024)

Kanko, R.M., Laende, E.K., Davis, E.M., Selbie, W.S., Deluzio, K.J.: Concurrent assessment of gait kinematics using marker-based and markerless motion capture. J. Biomech. 127, 110665 (2021). https://doi.org/10.1016/j.jbiomech.2021.110665

Kanko, R.M., Outerleys, J.B., Laende, E.K., Selbie, W.S., Deluzio, K.J.: Comparison of concurrent and asynchronous running kinematics and kinetics from marker-based motion capture and markerless motion capture under two clothing conditions, https://www.biorxiv.org/content/10.1101/2023.02.22.529537v3, (2023)

Kingma, I., de Looze, M.P., Toussaint, H.M., Klijnsma, H.G., Bruijnen, T.B.M.: Validation of a full body 3-D dynamic linked segment model. Hum. Mov. Sci. 15, 833–860 (1996). https://doi.org/10.1016/S0167-9457(96)00034-6

Kollia, A., Pillet, H., Bascou, J., Villa, C., Sauret, C., Lavaste, F.: Validation of a volumic model to obtain personalized body segment inertial parameters for people sitting in a wheelchair. Comput.

Methods Biomech. Biomed. Engin. 15, 208–209 (2012). https://doi.org/10.1080/10255842.2012.713701

de Leva, P.: Adjustments to Zatsiorsky-Seluyanov's segment inertia parameters. J. Biomech. 29, 1223–1230 (1996). https://doi.org/10.1016/0021-9290(95)00178-6

McAtamney, L., Nigel Corlett, E.: RULA: a survey method for the investigation of work-related upper limb disorders. Appl. Ergon. 24, 91–99 (1993). https://doi.org/10.1016/0003-6870(93)90080-S

Mehrizi, R., Peng, X., Metaxas, D.N., Xu, X., Zhang, S., Li, K.: Predicting 3-D Lower Back Joint Load in Lifting: A Deep Pose Estimation Approach. IEEE Trans. Hum.-Mach. Syst. 49, 85–94 (2019). https://doi.org/10.1109/THMS.2018.2884811

Mehrizi, R., Xu, X., Zhang, S., Pavlovic, V., Metaxas, D., Li, K.: Using a marker-less method for estimating L5/S1 moments during symmetrical lifting. Appl. Ergon. 65, 541–550 (2017). https://doi.org/10.1016/j.apergo.2017.01.007

Mohd Nur, N., Mohamed Salleh, M.A.S., Minhat, M., Mahmud Zuhudi, N.Z.: Load Lifting and the Risk of Work-Related Musculoskeletal Disorders among Cabin Crews. IOP Conf. Ser. Mater. Sci. Eng. 370, 012026 (2018). https://doi.org/10.1088/1757-899X/370/1/012026

Nérot, A., Choisne, J., Amabile, C., Travert, C., Pillet, H., Wang, X., Skalli, W.: A 3D reconstruction method of the body envelope from biplanar X-rays: Evaluation of its accuracy and reliability. J. Biomech. 48, 4322–4326 (2015). https://doi.org/10.1016/j.jbiomech.2015.10.044

Newell, A., Yang, K., Deng, J.: Stacked Hourglass Networks for Human Pose Estimation. Presented at the , Cham (2016)

Pillet, H., Bonnet, X., Lavaste, F., Skalli, W.: Evaluation of force plate-less estimation of the trajectory of the centre of pressure during gait. Comparison of two anthropometric models. Gait Posture. 31, 147–152 (2010). https://doi.org/10.1016/j.gaitpost.2009.09.014

Robert, T., Leborgne, P., Abid, M., Bonnet, V., Venture, G., Dumas, R.: Whole body segment inertia parameters estimation from movement and ground reaction forces: a feasibility study. Comput. Methods Biomech. Biomed. Engin. 20, S175–S176 (2017). https://doi.org/10.1080/10255842.2017.1382919

Sandoz, B., Laporte, S., Skalli, W., Mitton, D.: Subject-specific body segment parameters' estimation using biplanar X-rays: a feasibility study. Comput. Methods Biomech. Biomed. Engin. 13, 649–654 (2010). https://doi.org/10.1080/10255841003717608

Skals, S., Bláfoss, R., Andersen, M.S., de Zee, M., Andersen, L.L.: Manual material handling in the supermarket sector. Part 1: Joint angles and muscle activity of trapezius descendens and erector spinae longissimus. Appl. Ergon. 92, 103340 (2021). https://doi.org/10.1016/j.apergo.2020.103340

Song, K., Hullfish, T.J., Scattone Silva, R., Silbernagel, K.G., Baxter, J.R.: Markerless motion capture estimates of lower extremity kinematics and kinetics are comparable to marker-based across 8 movements. J. Biomech. 157, 111751 (2023). https://doi.org/10.1016/j.jbiomech.2023.111751

Swain, C.T.V., Pan, F., Owen, P.J., Schmidt, H., Belavy, D.L.: No consensus on causality of spine postures or physical exposure and low back pain: A systematic review of systematic reviews. J. Biomech. 102, 109312 (2020). https://doi.org/10.1016/j.jbiomech.2019.08.006

Tang, H., Munkasy, B., Li, L.: Differences between lower extremity joint running kinetics captured by marker-based and markerless systems were speed dependent. J. Sport Health Sci. (2024). https://doi.org/10.1016/j.jshs.2024.01.002

Vafadar, S., Skalli, W., Bonnet-Lebrun, A., Assi, A., Gajny, L.: Assessment of a novel deep learning-based marker-less motion capture system for gait study. Gait Posture. 94, 138–143 (2022). https://doi.org/10.1016/j.gaitpost.2022.03.008

421 Vafadar, S., Skalli, W., Bonnet-Lebrun, A., Khalifé, M., Renaudin, M., Hamza, A., Gajny, L.: A novel
422 dataset and deep learning-based approach for marker-less motion capture during gait. Gait Posture. 86,
423 70–76 (2021). https://doi.org/10.1016/j.gaitpost.2021.03.003
424 Venture, G., Bonnet, V., Kulic, D.: Creating Personalized Dynamic Models. In: Venture, G., Laumond,
425 J.-P., and Watier, B. (eds.) Biomechanics of Anthropomorphic Systems. pp. 91–104. Springer
426 International Publishing, Cham (2019)

427